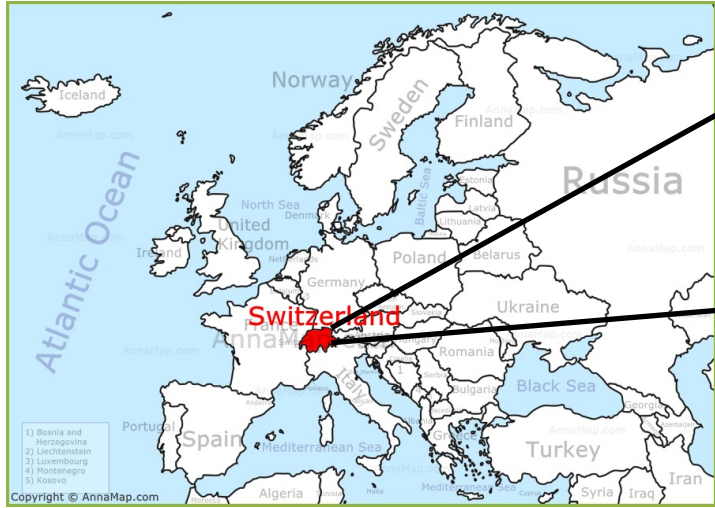


Simulations of stellarator boundary turbulence in the space of magnetic geometries

Joaquim Loizu, António Coelho, Zeno Tecchiolli, Maurizio Giacomin, Paolo Ricci

Where are we, behind the screen

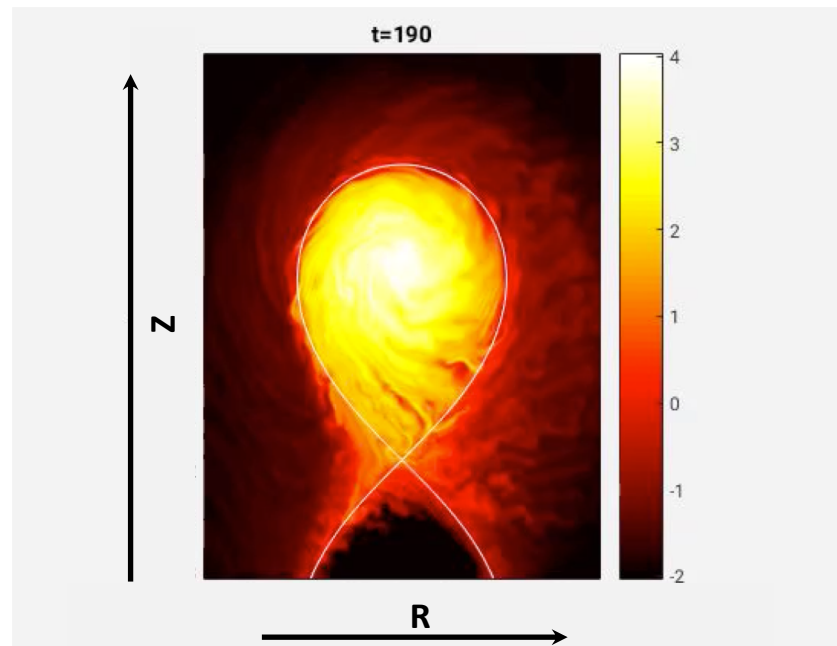


As tokamaks, stellarators need to address the issue of how to best exhaust heat and particles.

Goals concerning power exhaust:

- ❖ exhaust power without damaging materials
→ radiate and spread the heat on target
- ❖ maintain core performance
→ control impurity dilution and ionization/radiation fronts
- ❖ allow easy pumping of neutrals
→ maximize neutral pressure close to target

Important player in this game is **turbulence!**



GBS simulation of plasma turbulence in a tokamak with a single null

Braginskii [Reviews of Plasma Physics, 1965] derived, starting from kinetic theory, a set of fluid equations that is asymptotically valid in the limit of high plasma collisionality ($\nu^* \gg 1$) and thus adequate in the 'cold boundary'.

continuity
$$\frac{\partial n_\alpha}{\partial t} + \nabla \cdot (n_\alpha \mathbf{V}_\alpha) = 0$$

momentum
$$m_\alpha n_\alpha \frac{d_\alpha \mathbf{V}_\alpha}{dt} = -\nabla p_\alpha - \nabla \cdot \underline{\underline{\pi_\alpha}} + e_\alpha n_\alpha (\mathbf{E} + \mathbf{V}_\alpha \times \mathbf{B}) + \mathbf{R}_\alpha$$

energy
$$\frac{3}{2} n_\alpha \frac{d_\alpha T_\alpha}{dt} = -p_\alpha \nabla \cdot \mathbf{V}_\alpha - \nabla \cdot \mathbf{q}_\alpha + Q_\alpha^{visc} + Q_\alpha$$

... + Maxwell equations

~ viscosity (pointing to $\underline{\underline{\pi_\alpha}}$)

~ resistivity (pointing to \mathbf{R}_α)

~ heat conductivity (pointing to \mathbf{q}_α)

Braginskii equations describe the plasma dynamics on time scales ranging from $\Omega_{ce}^{-1} \sim 10^{-11} \text{ s}$ up to $\tau_E \sim 1 \text{ s}$.

Zeiler [IPP report 5/88, 1999] derived, starting from Braginskii equations, a reduced set of equations valid in the limit of “low-frequency” ($\omega \ll \Omega_{ci}$) and “large scale” turbulence ($(k_{\perp} \rho_s)^2 \ll 1$) thus adequate in the boundary.

For example, in the cold ion ($T_i = 0$) electrostatic limit ($\partial_t B = 0$):

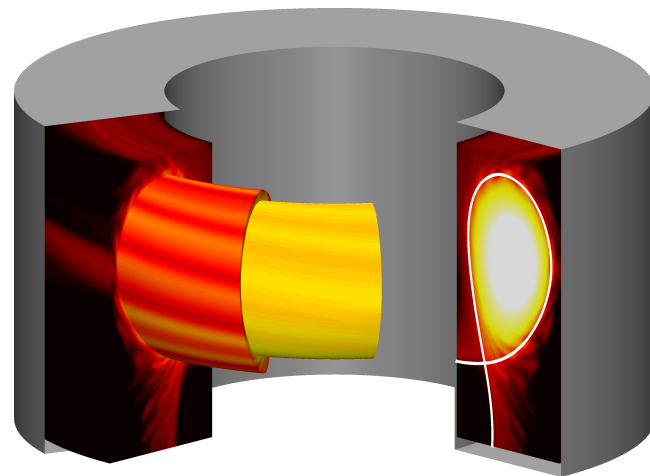
electron continuity	$\frac{\partial n}{\partial t} = -\nabla \cdot [n(\mathbf{V}_E + \mathbf{V}_{de} + V_{\parallel e} \mathbf{b})] ,$	\nearrow ~ drive for curvature-driven modes
charge conservation	$\nabla \cdot \left(\frac{en}{B\omega_{ci}} \frac{d_{i0}}{dt} \nabla_{\perp} \phi \right) = \nabla_{\parallel} j_{\parallel} - \nabla \cdot (en \mathbf{V}_{de}) ,$	\nearrow ~ destabilizes drift-waves
electron momentum	$m_e n \frac{d_{e0} V_{\parallel e}}{dt} = -\nabla_{\parallel} p_e + en \nabla_{\parallel} \phi - 0.71 n_e \nabla_{\parallel} T_e + en_e \nu_{\parallel} j_{\parallel} - \frac{2}{3} \nabla_{\parallel} G_e$	
ion momentum	$m_i n \frac{d_{i0} V_{\parallel i}}{dt} = -\nabla_{\parallel} p_e ,$	
electron energy	$\frac{3}{2} n_e \frac{d_e T_e}{dt} = -p_e \nabla \cdot \mathbf{V}_e + 0.71 \frac{T_e}{e} \nabla_{\parallel} j_{\parallel} + \chi_{\parallel e} \nabla_{\parallel}^2 T_e + \nabla \cdot \left(\frac{5 n T_e}{2 e B} \mathbf{b} \times \nabla T_e \right)$	

The Global Braginskii Solver (GBS) [Giacomin, JCP 2022] developed over the last ~ 15 years:

- solves **Zeiler's equations** in a toroidal domain of rectangular cross-section,
- given an equilibrium \mathbf{B} , 2D or 3D, with arbitrary magnetic topology [Coelho et al, NF 2022],
- given density and temperature **sources**,
- with **sheath** boundary conditions [Loizu et al, PoP 2012],
- with coupling to a kinetic neutral model [Mancini et al, NF 2024].

Quasi-steady state = balance between source, turbulence, sheath losses

Cross-validation of turbulence codes (GBS, GRILLIX, TOKAM3X) with experiments on TCV has been carried out [Oliveira et al, NF 2022].



GBS simulation of TCV shot #65402 @1s

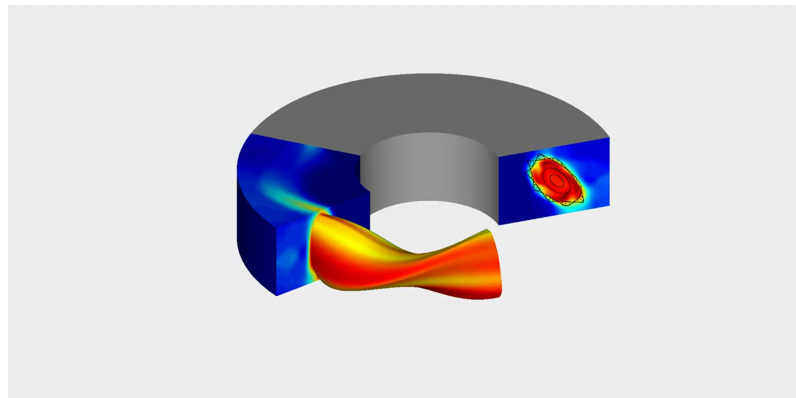
[M. Giacomin, PhD thesis 2022]

GBS numerical scheme includes:

- Explicit time-advance using Runge-Kutta fourth-order scheme,
- Spatial derivatives evaluated with fourth-order finite difference scheme,
- Arakawa scheme for the Poisson brackets (\mathbf{ExB} advection),
- Density and velocity grids are staggered in two directions,
- MPI parallelization in (x,y,z) with z the 'toroidal direction'.

Typical stellarator simulation on JFRS-1:

- Grid size $(n_x, n_y, n_z) \sim (200)^3$,
- 1 node per few (x,y) planes, total of ~ 40 nodes,
- Simulation time $\sim 50'000$ node-hours.

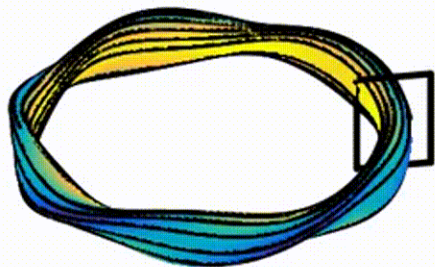


[Coelho et al, NF 2022]

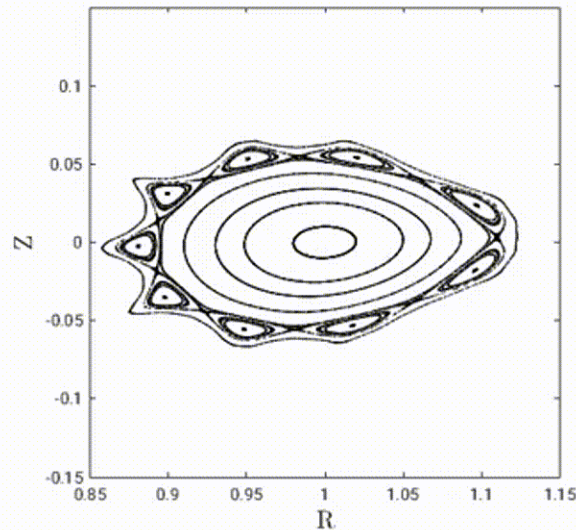
A stellarator vacuum field can be described by a potential satisfying Lapace's equation.

$$\nabla \times \mathbf{B} = 0 \quad \mathbf{B} = \nabla V$$

$$\nabla \cdot \mathbf{B} = 0 \quad \nabla^2 V = 0$$

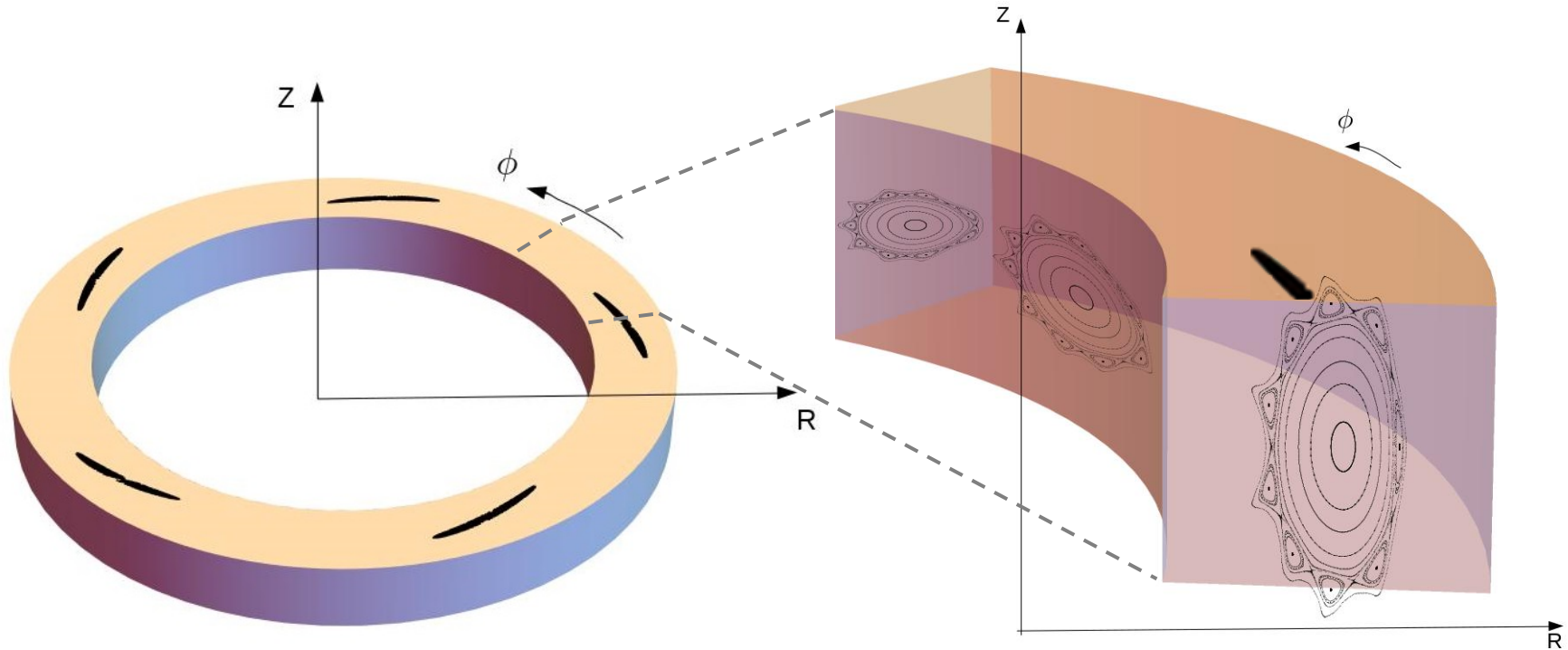


$$V(R, \phi, Z) = \phi + \sum_{m,l} V_{m,l}(R, \phi, Z)$$

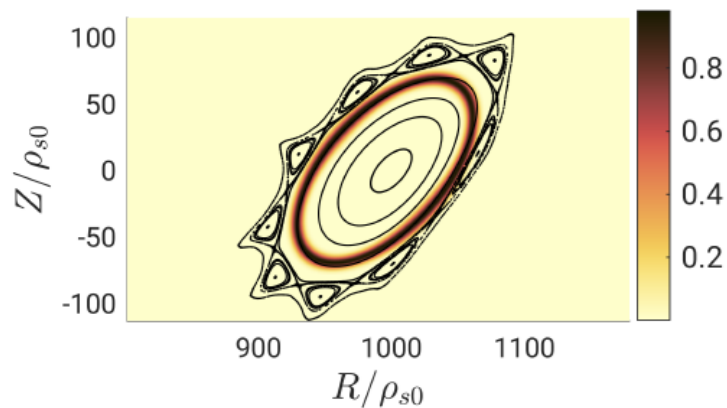
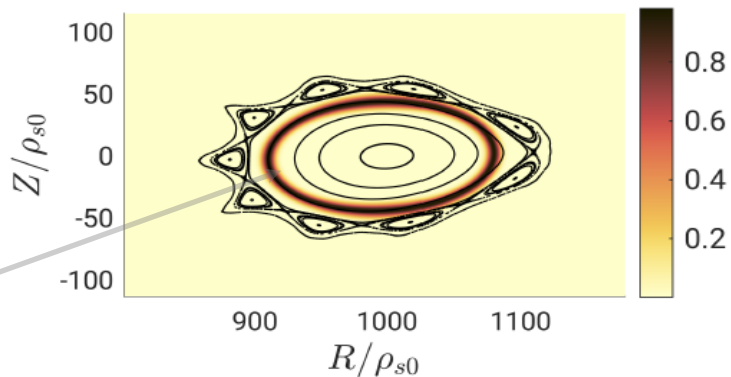


Dommasck potentials [Dommaschk, CPC 1986] form complete basis for the vacuum solution in a torus.

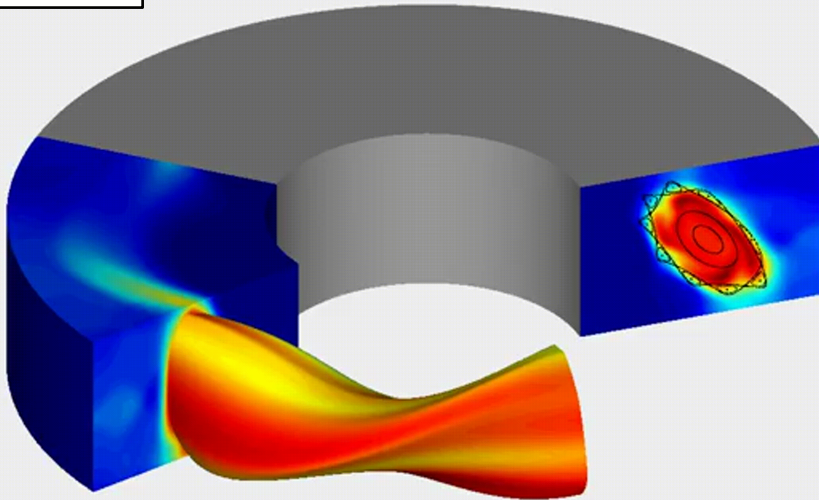
We shape the wall so that islands intersect top/bottom



$$\frac{\partial n}{\partial t} + \nabla \cdot \Gamma_{\text{ExB}} + \nabla \cdot \Gamma_{\text{dia}} + \nabla \cdot \Gamma_{\parallel e} = \mathcal{S}_n$$

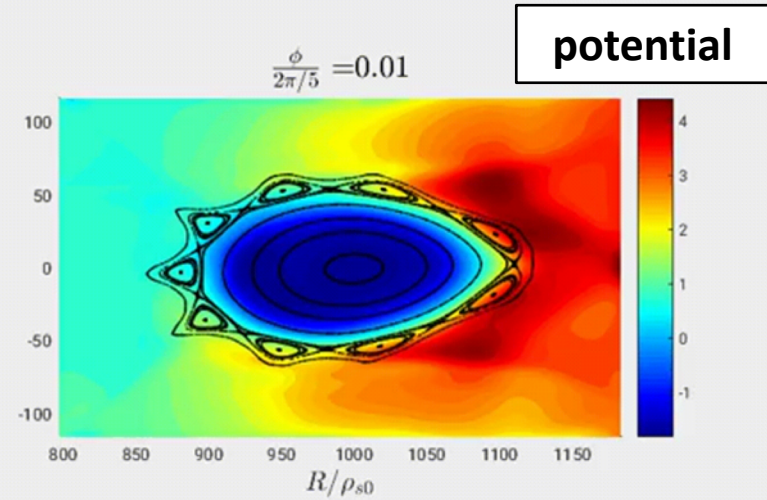
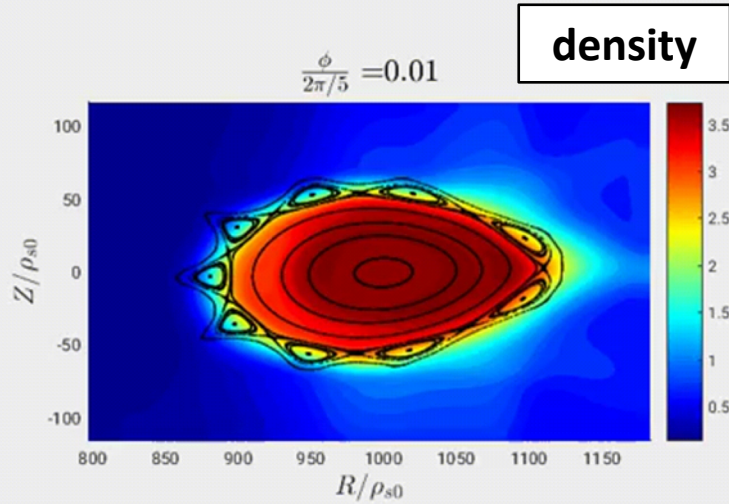


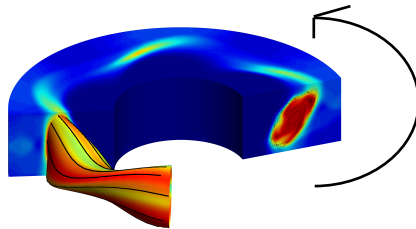
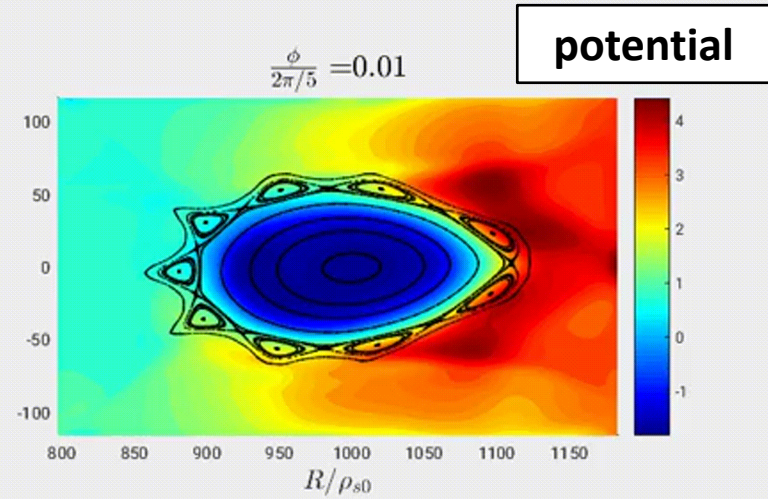
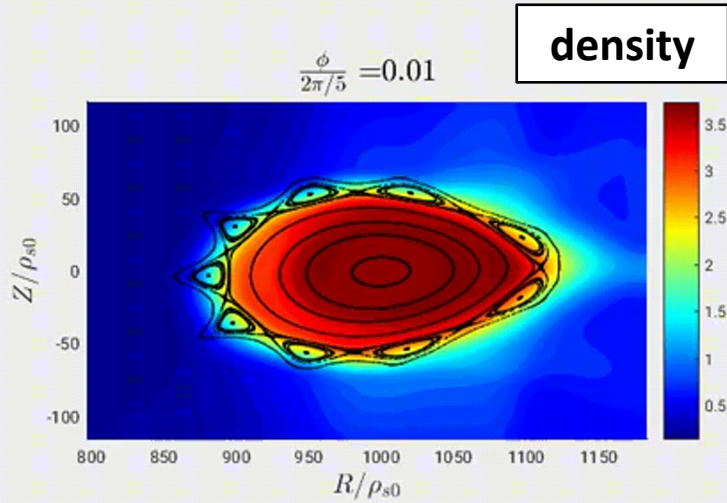
density



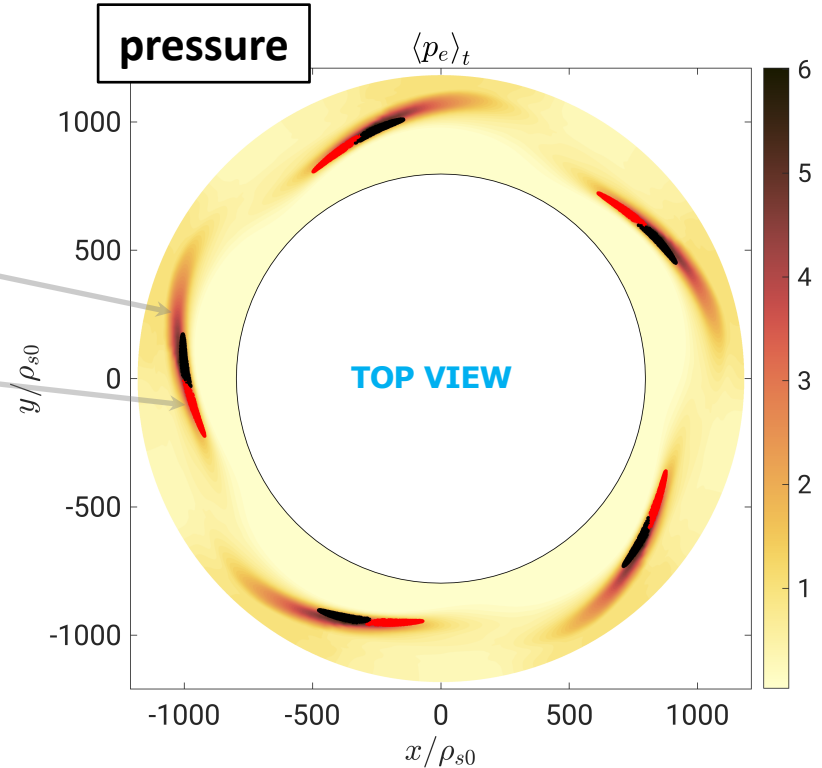
equilibrium $\rightarrow \langle f \rangle_t$

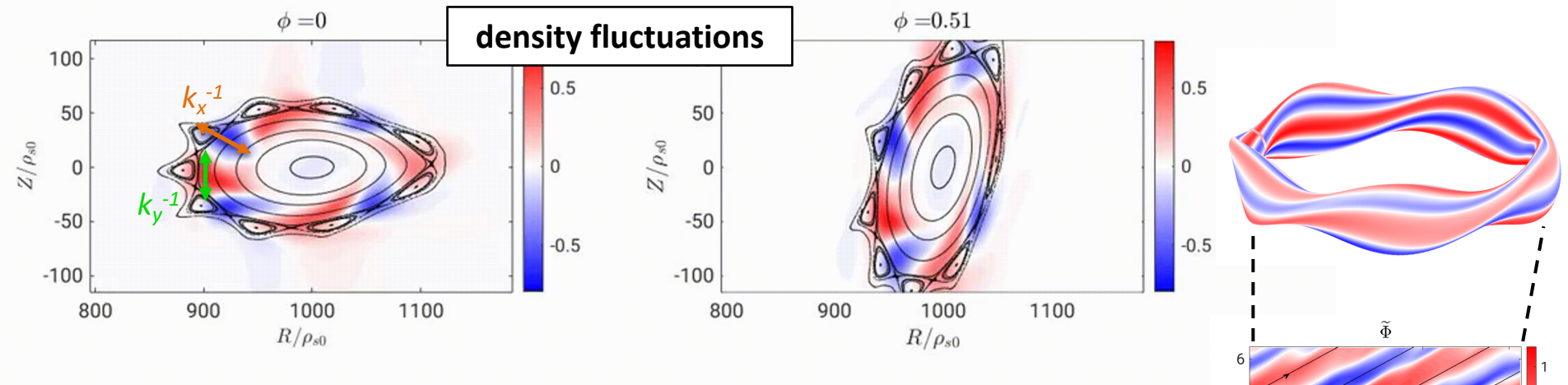
fluctuations $\rightarrow \tilde{f} = f - \langle f \rangle_t$





- The heat deposition pattern on the targets is as expected from the footprints of the islands.

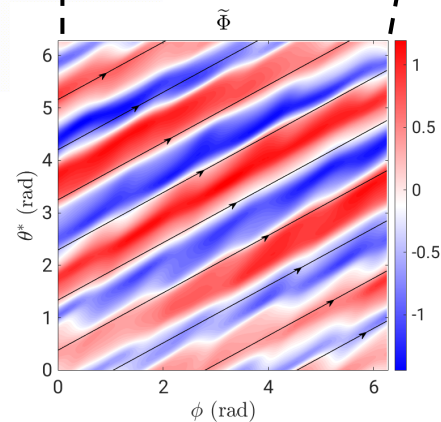




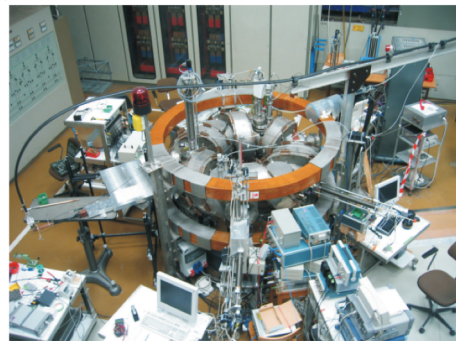
- $m = 4, n = 2$ mode with $k_x \rho_s \sim k_y \rho_s \sim 0.04$ dominates dynamics
- mode retrieved with nonlocal linear theory [Coelho et al, NF 2022]
- highlights importance of geodesic curvature:

$$\gamma^2 + \frac{1}{\nu n_0} \left(\frac{k_{\parallel}}{k_{\perp}} \right)^2 \gamma = 2\rho_*^{-1} \frac{k_y^2}{k_{\perp}^2} \left(\frac{T_{e0}}{n_0} \frac{\partial n_0}{\partial x} + \frac{\partial T_{e0}}{\partial x} \right) \left(\text{sign}(B_{\phi}) \frac{k_x}{k_y} \kappa_g + \kappa_n \right)$$

- mode breaks the discrete symmetry of the stellarator! [Coelho et al, submitted to NF]

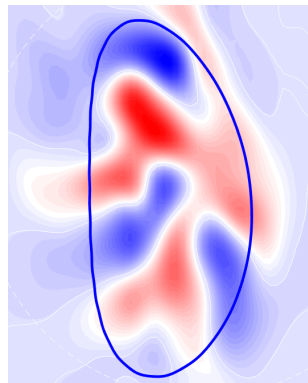
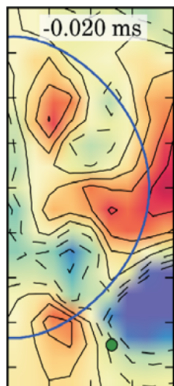


[Coelho et al, PPCF 2023]

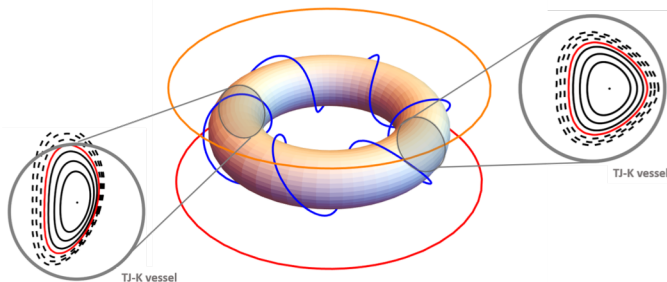
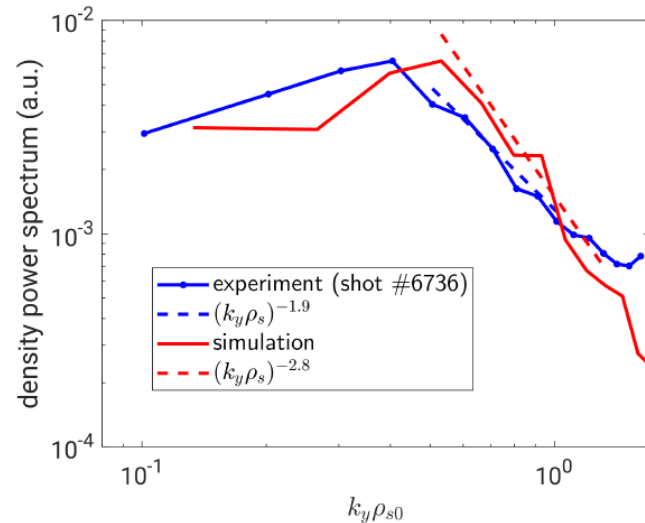


TJ-K stellarator (6-field period)

density fluct. - experiment density fluct. - simulation



[Fuchert et al, PPCF 2013]

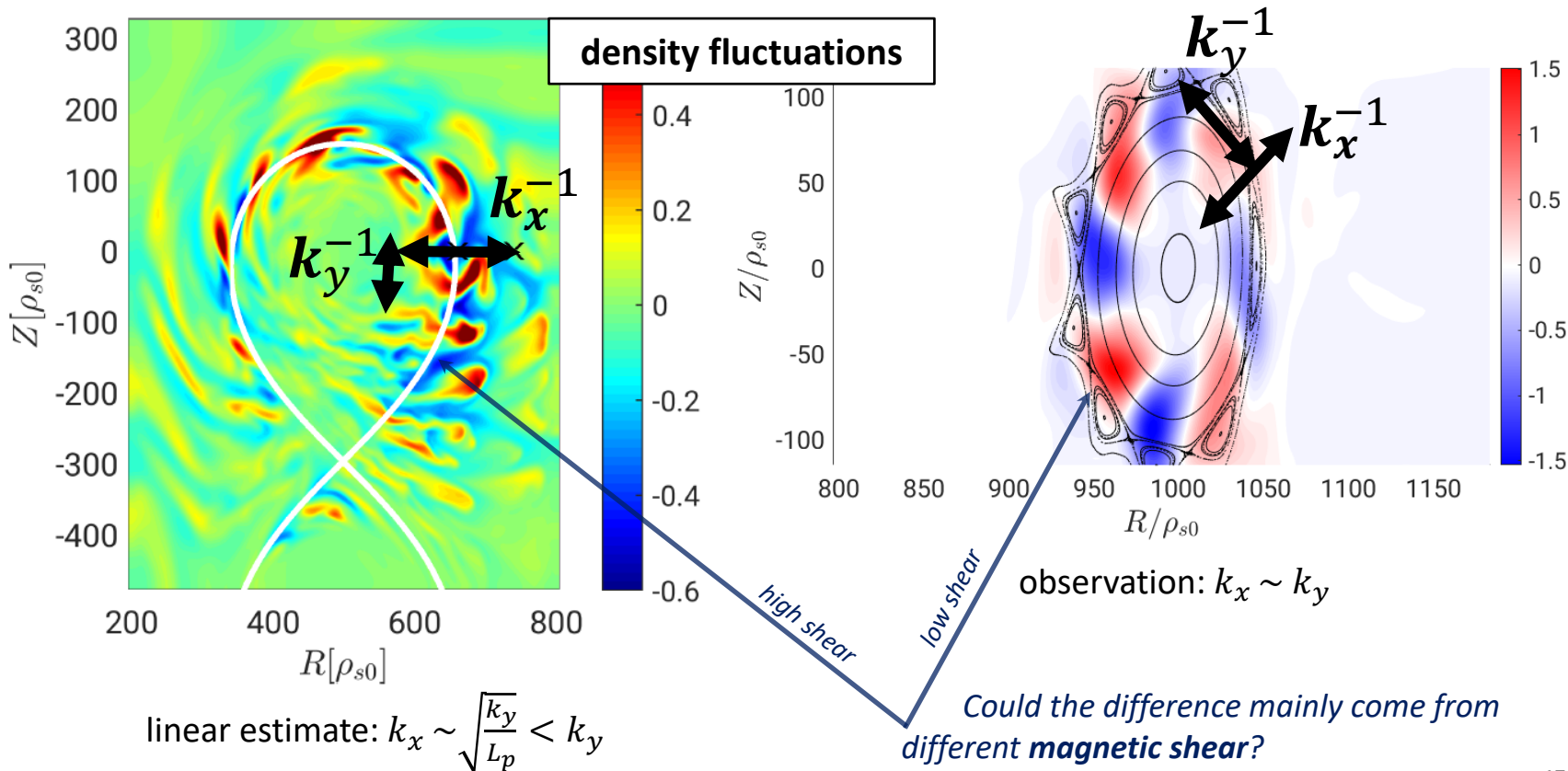


Used GBS code to simulate plasma dynamics in TJ-K with real sources.

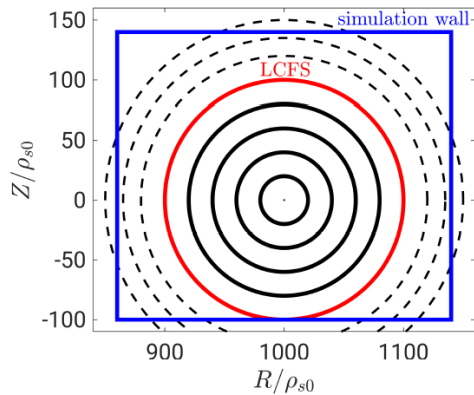
Model valid in whole device (except no neutral physics included).

Reproduced the fluctuations spectrum, dominant $m=4, n=1$ mode.

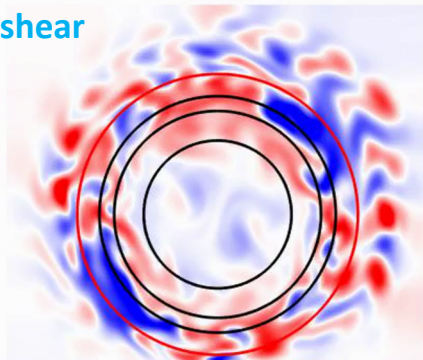
Differences between tokamak/stellarator simulations might be explained by magnetic shear



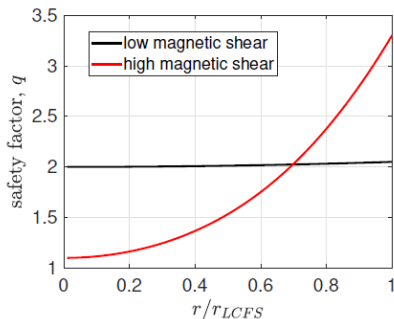
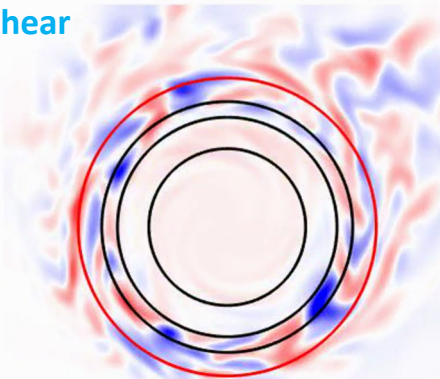
[Tecchioli et al, in preparation]



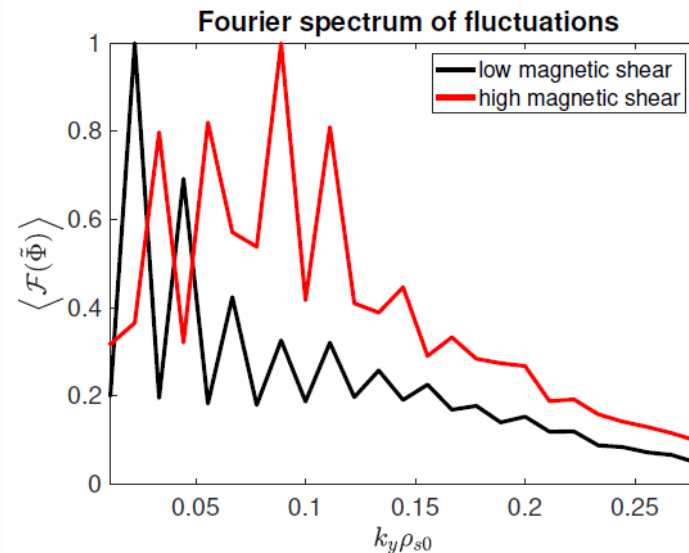
low shear



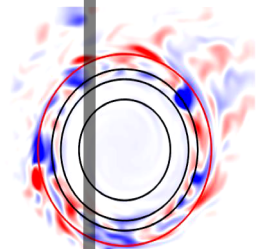
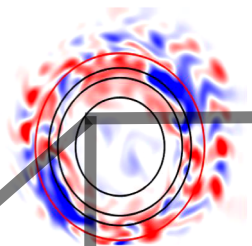
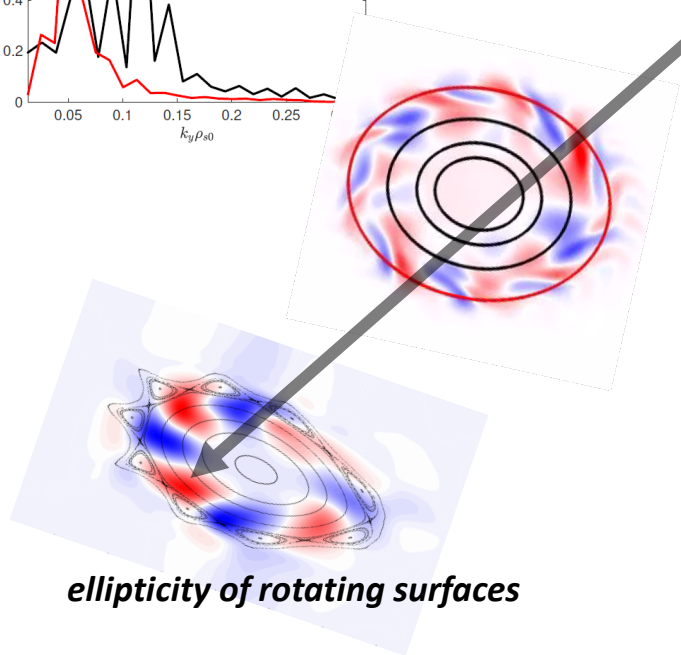
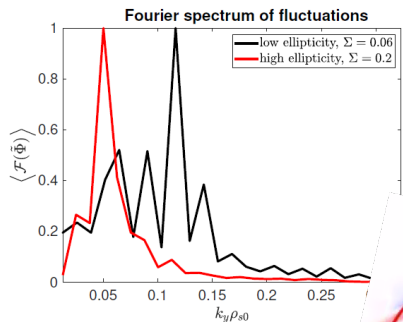
high shear



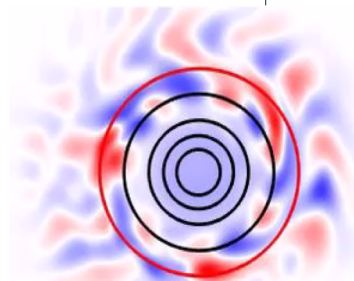
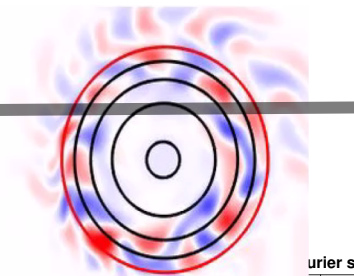
two circular tokamak configurations



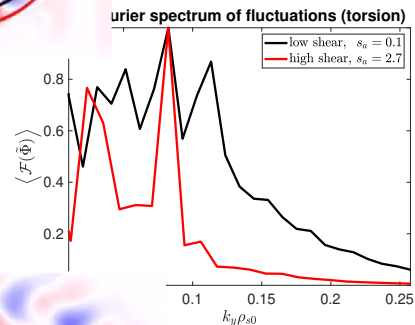
We explored the effect of ellipticity and torsion



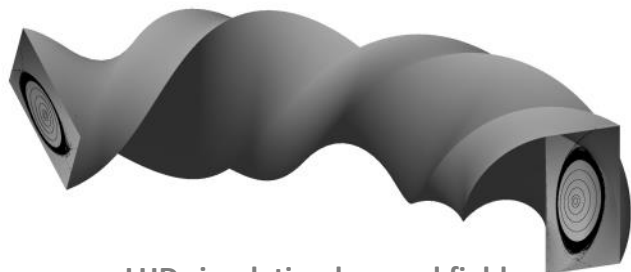
magnetic shear



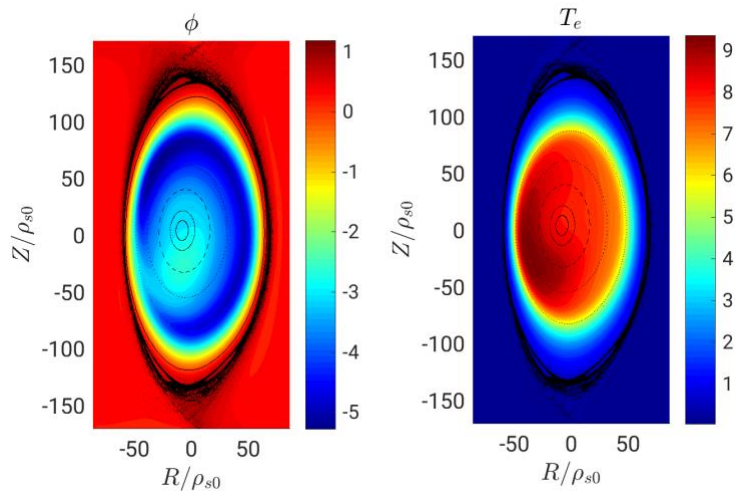
axis torsion



- ❖ LHD has high-shear, high ellipticity, small torsion: what is the nature of boundary turbulence?
- ❖ We might be able to reproduce soft density limits as observed experimentally.
- ❖ Including the **neutral physics** in the simulations might allow studying detachment.



LHD simulation box and field



- ❖ GBS is the first code to carry out a global simulation of boundary fluid turbulence in a stellarator.
- ❖ Low- m coherent modes that break stellarator periodicity tend to develop, at least in low-shear.
- ❖ We have reproduced the fluctuation spectrum in the TJ-K stellarator experiment.
- ❖ We have explored the effect of global shear, axis-torsion, and near-axis-ellipticity on turbulence.
- ❖ We are currently simulating realistic large-scale configurations such as LHD, but also W7-AS.